THE JOURNAL OF PHYSICAL CHEMISTRY B

Article

pubs.acs.org/JPCB

Ionic Transport in Polymer Electrolytes Based on PEO and the PMImI Ionic Liquid: Effects of Salt Concentration and Iodine Addition

Tobias Eschen,[†] Johannes Kösters,[†] Monika Schönhoff,[‡] and Nicolaas A. Stolwijk*,[†]

[†]Institut für Materialphysik, University of Münster, Wilhelm-Klemm-Str. 10, 48149 Münster, Germany

[‡]Institut für Physikalische Chemie, University of Münster, Corrensstr. 28/30, 48149 Münster, Germany

ABSTRACT: We find a strong impact of ion pairing on ionic transport in potential Grätzel-cell electrolytes based on poly(ethylene oxide) (PEO) and 1-propyl-3-methylimidazolium iodide (PMImI). Furthermore, the addition of free iodine enhances both mass and charge transport, which can be explained by the reduced pair-formation tendency of the bulky triiodide ion. These results arise from conductivity and diffusion measurements on amorphous complexes with EO/PMImI molar ratios of 20 and 30 and their evaluation in a comprehensive ion-transport model. In particular, the charge diffusivity D_σ was compared with the PMIm diffusivity D^*_{cat} determined by pulsed-field-gradient nuclear magnetic resonance and the iodine diffusivity D^*_{an} obtained from radiotracer depth profiling. Simultaneous fitting of these diffusion coefficients in complexes with and without iodine additive yields best values for the model parameters. The results characterize not only the mobility of free ions and pairs as a function of temperature and composition but also the degree of ion pairing.

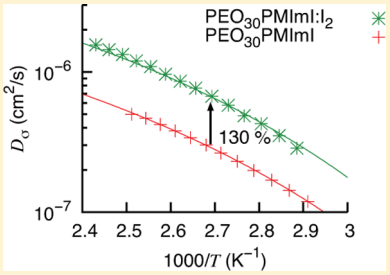

1. INTRODUCTION

In this paper, we investigate ionic transport in solid polymer electrolytes (SPEs) that are based on a polymer matrix complexed with an ionic liquid instead of an inorganic salt. Ionic liquids (ILs) are concentrated salt systems usually consisting of a complex organic cation and a conventional inorganic anion, which have their melting point below or slightly above room temperature.[1] Outstanding IL properties are—among other factors—a very low vapor pressure and a high ionic conductivity, which make them promising for application in batteries and dye-sensitized solar cells (DSSCs).[2,3] By dissolving these salts in a polymer matrix, we synthesize an electrolyte that combines the advantages of high conductivity in ILs and a mechanically flexible solid-like state typical for SPEs.[4,5]

Our investigation focuses on the ion-transport properties in SPE-IL complexes with potential application to DSSCs. This solar cell type relies on the light-induced excitation of dye molecules and the subsequent electron transfer across the conduction band of TiO_2 nanoparticles toward the transparent working electrode.[6] The circuit is closed by a counter electrode and an appropriate electrolyte layer, which allows for the recovery of the dye molecules. This is commonly achieved through a I_1^-/I_3^- redox couple and the migration of the ionic species involved. Therefore, electrolytes for DSSCs require the use of an iodide as salt component and also the addition of small amounts of free I_2 in order to produce I_3^- from the reaction with the abundant I_1^- ions.[6] In this context, both the salt (or iodide) concentration and the amount of added I_2 are crucial parameters for the performance of DSSC electrolytes.[7,8]

The present study concerns complexes of poly(ethylene oxide) (PEO) and 1-propyl-3-methylimidazolium iodide (PMImI), which have been previously investigated as DSSC electrolytes.[9] In particular, both mass and charge transport in PEO_{20}PMImI and PEO_{30}PMImI are characterized as a function of temperature, where the composition index 20 or 30 specifies the EO/cation mole ratio. To this aim, the total ionic conductivity is measured by electrical impedance spectroscopy (EIS), whereas the diffusivity of the PMImI cations results from analysis with pulsed-field-gradient nuclear magnetic resonance (PFG-NMR). A special feature of this work is the direct determination of iodine transport via ^{125}I radiotracer diffusion (RTD). It should be noted that PFG-NMR is not suitable to resolve the diffusivity of iodine.

The unique combination of EIS with PFG-NMR and RTD provides a virtually complete experimental picture of ionic transport in PEO−PMImI complexes. This is not only true for the base complexes PEO_{20}PMImI and PEO_{30}PMImI but also for the doped complexes PEO_{20}PMImI:I_2 and PEO_{30}PMImI:I_2 which contain a certain amount of I_2 (to be specified below). In addition to the presentation of the experimental results, this paper includes an in-depth theoretical analysis of the measured data based on a comprehensive ion-transport model described in earlier publications.[10−12] This analysis does not only reveal the impact of neutral ion pairs on mass and charge transport but also yields some fundamental characteristics of the electrolytes investigated, e.g., the pair-formation enthalpy and entropy and the mobility of individual ionic species.

Specifically, it will be shown that the effects of I_2 addition on ionic conductivity and diffusivity can be explained by the much weaker ion-pairing tendency of I_3^- with respect to I_1^-. This conclusion for PEO−IL complexes supports the results of an

Received: April 13, 2012
Revised: June 20, 2012
Published: June 21, 2012

   dx.doi.org/10.1021/jp303579b | J. Phys. Chem. B 2012, 116, 8290−8298

earlier study by our group on the conventional $PEO_{30}NaI:I_2$ complex.[11] Moreover, the present work appears to confirm that in dilute iodide-based electrolytes in contrast to concentrated ones there is no need to invoke an additional Grotthuss-like diffusion mechanism to rationalize the observed ion-transport behavior.[13−15]

2. EXPERIMENTAL SECTION

2.1. Materials and Preparation. The base materials were PEO with a molecular weight of 8×10^6 g/mol and a purity of 98.4 wt %[16] (Aldrich), PMImI (252.1 g/mol, 99.9 wt %, IoLiTec), and iodine (253.8 g/mol, 99.999 wt %, Sigma-Aldrich). For the preparation of the polymer electrolytes the same methods were used as described in earlier publications by our group.[11,17] Four complexes were investigated, with two of them containing additional I_2. The complexes $PEO_{20}PMImI$ and $PEO_{20}PMImI:I_2$ are richer in salt than $PEO_{30}PMImI$ and $PEO_{30}PMImI:I_2$, in accordance with the given values of the mole ratio index y = EO/PMImI. The two complexes with additional I_2 are more completely labeled as $PEO_yPMImI:I_2$ (1:z), where z = 1/4 denotes the fixed mole fraction of I_2 to PMImI.

2.2. Electrolyte Characterization. The mass density of the electrolytes was determined by hydrostatic weighing in dodecane and air, taking single-crystal silicon as reference material. The density enters the calculation of the salt concentration per unit volume. Phase behavior was examined by differential scanning calorimetry (DSC) at different heating and cooling rates using Perkin-Elmer DSC-7 equipment.

2.3. Impedance Spectroscopy. The ionic conductivity was measured by impedance spectroscopy in the frequency range from 5 Hz to 13 MHz using a HP Agilent 4192A LF impedance analyzer.[18] The measurements were done with at least two different samples for each composition and for multiple heating and cooling circles. As ionic conduction mainly takes place in the amorphous phase of the electrolytes, the data covered the widest possible temperature range of this phase. In practice, this range extended from the common lower limit of 70 °C to a variable upper limit between 120 and 160 °C depending on electrolyte composition.

2.4. Pulsed-Field-Gradient Nuclear Magnetic Resonance. The cation diffusivity D^*_{cat} was measured by PFG-NMR of ^1H nuclei bound to the PMIm structure using a Bruker 400 MHz Avance NMR spectrometer. The intensity I of the echo signal decreases with increasing strength of the magnetic-field gradient g according to[19]

$$I = I_0 \exp\left(-\gamma^2 g^2 \delta^2 D^*_{cat}\left(\Delta - \frac{\delta}{3}\right)\right) \quad (1)$$

Here I_0 denotes the zero-gradient intensity, γ is the gyromagnetic ratio, δ is the duration of the gradient pulse, and Δ is the effective diffusion time related to the delay times in the pulse sequence. The cation has seven different types of protons leading to evaluable resonance peaks at four different frequencies. In principle, each peak can be used to calculate a diffusion coefficient, so that each measurement at a single temperature yielded four values of D^*_{cat}, which mutually agreed within 20%. The resulting data, to be presented and analyzed below, are the mean values of these four single-peak diffusion coefficients. A fifth ^1H peak appearing in the spectrum is only weakly attenuated by the field gradient and is therefore interpreted as the signal from the PEO chains.

2.5. Radiotracer Diffusion. The anion diffusivity D^*_{an} was measured by the RTD method, which is described in detail elsewhere.[12] The radionuclide ^{125}I with a half-life of 60 days was used as iodine tracer. After placing a radioactive source film on top of a sample and a subsequent annealing treatment in an oil bath at constant temperature, the sample was sectioned with a rotary microtome. A depth profile of ^{125}I was obtained by counting the radioactivity in each section. D^*_{an} was calculated by fitting the appropriate solution of Fick's second law to the measured penetration profile given by[12]

$$c(x, t) = \frac{1}{2} c_0 \left[\mathrm{erfc}\left(\frac{x}{2\sqrt{D^*_{an} t}}\right) + \mathrm{erfc}\left(\frac{x + 2h}{2\sqrt{D^*_{an} t}}\right)\right] \quad (2)$$

Here, c_0 denotes the tracer concentration (activity) of the source layer of width h and $c(x,t)$ is the corresponding value at depth x after diffusion time t. For extremely low and high values of $h/(D^*_{an}t)^{1/2}$, eq 2 converges to the Gaussian and complementary error function, respectively. In contrast to PFG-NMR, the RTD technique is destructive, so that each measurement requires a new sample.

3. EXPERIMENTAL RESULTS

Upon heating in the EIS measuring cell or DSC detector head, all four compositions become amorphous at a temperature of about 63 °C, which is close to the melting temperature of pure PEO. For $PEO_{20}PMImI$ and $PEO_{30}PMImI$, the conductivity was found to decrease strongly with increasing temperature above ∼120 °C, which can be explained by salt precipitation. This explanation is supported by DSC measurements (not shown here) exhibiting an endothermic event upon heating at the same temperature. Such effects were not observed for the complexes with I_2, which indicates that the addition of iodine stabilizes the PEO_yPMImI electrolytes. For these reasons, the analysis of the experimental data was limited to the temperature range of 70−120 °C for $PEO_{20}PMImI$ and $PEO_{30}PMImI$ and to the extended range of 70 −160 °C for $PEO_{20}PMImI:I_2$ and $PEO_{30}PMImI:I_2$.

Figure 1 shows the ionic conductivity of the four investigated electrolytes as Arrhenius plots. Not surprisingly, the conductivity appears to increase with increasing temperature. The temperature dependence can be fitted (solid lines) by the Vogel−Tammann−Fulcher (VTF) equation

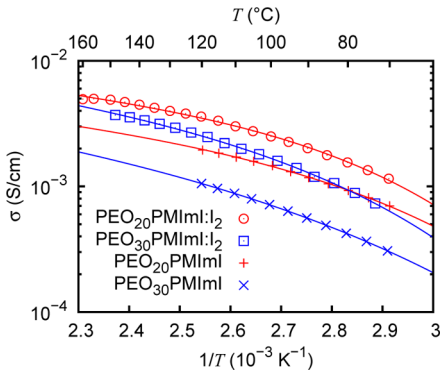

Figure 1. The dc conductivity of PEO_yPMImI and $PEO_yPMImI:I_2$ electrolytes for two different monomer/salt molar ratios y as a function of inverse temperature. The solid lines are fits based on the VTF expression (cf. eq 3).

dx.doi.org/10.1021/jp303579b | J. Phys. Chem. B 2012, 116, 8290−8298

$$\sigma_{dc}(T) = \sigma_0 \exp\left(-\frac{B_\sigma}{T - T_{\sigma 0}}\right) \quad (3)$$

Here σ_0 denotes a pre-exponential factor, T is temperature, $T_{\sigma 0}$ is a reference temperature, at which the ionic mobility vanishes, and B_σ is an "activation temperature" or pseudo activation energy. It should be mentioned, however, that no physical meaning is attributed to the parameter values obtained by the fitting with eq 3. Rather, the solid lines in Figure 1 serve to guide the eye.

The conductivity in $PEO_{20}PMImI$ is found to be significantly higher than in $PEO_{30}PMImI$, which is consistent with the difference in ion concentration between the two complexes. Furthermore, the addition I_2 of leads to a distinct increase of the conductivity in both electrolytes as demonstrated by the data on $PEO_{20}PMImI:I_2$ and $PEO_{30}PMImI:I_2$ in Figure 1. This seems surprising, since I_2 is not an ionic species. However, an explanation for this crucial finding will be given in section 5.

By using the Nernst−Einstein equation, it is possible to convert the conductivity into a diffusion coefficient, i.e., the charge diffusivity D_σ. In this work, we use the specific form

$$D_\sigma = \frac{k_B T}{C_{salt} e^2} \sigma \quad (4)$$

where k_B denotes the Boltzmann constant and e is elementary charge. It is noteworthy that eq 4 contains the known salt concentration C_{salt} (number density of molecules) instead of the unknown concentration of free (dissociated) ions. This allows us to treat D_σ as an experimental quantity that can be directly compared with the other measured diffusion coefficients D^*_{cat} and D^*_{an}, as demonstrated in Figures 4 and 5 to be discussed later on. It should be emphasized that this very comparison makes it feasible to deduce the degree of dissociation as a characteristic feature of the electrolyte systems under investigation (cf. section 5).

In Figure 2, the normalized intensity of the PFG-NMR signal of $PEO_{30}PMImI:I_2$ is displayed as a function of g^2 for different

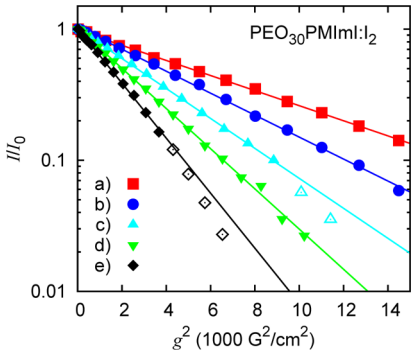

Figure 2. Normalized PFG-NMR echo intensities of the strongest ^1H signal as a function of the magnetic-field strength g. The data result from $PEO_{30}PMImI:I_2$ at different temperatures: (a) 70, (b) 80, (c) 90, (d) 100, and (e) 110 °C. Open symbols have been ignored in the exponential-decay fits (solid lines).

temperatures. The data of the largest ^1H peak associated with the highest resonance frequency are plotted. According to eq 1, the T dependence of the cation diffusivity is reflected by the differences in slope of the straight lines fitted to the experimental data (closed symbols). In the fitting procedure, some data points at lower intensities (open symbols) were neglected. As indicated above, the D^*_{cat} data originating from different ^1H peaks are mutually consistent. The pertaining mean values are displayed in Figures 4 and 5 as slanted crosses (×).

Figure 3 displays two typical depth profiles of ^{125}I in $PEO_{20}PMImI:I_2$ to illustrate the prime results obtained by the

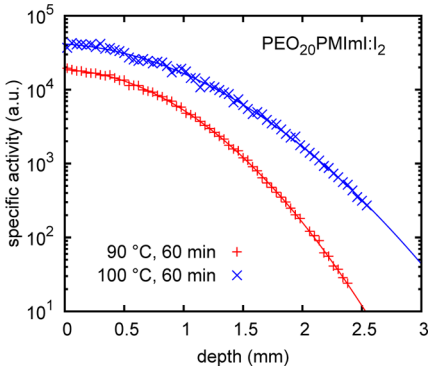

Figure 3. Depth profiles of the ^{125}I specific activity in $PEO_{20}PMImI:I_2$ measured after diffusion treatments at temperatures and for times as indicated.

radiotracer technique. The profiles extend over more than 2 orders of magnitude in specific activity and over more than 2 mm in penetration depth. The solid lines are least-squares fits based on eq 2, showing virtual perfect coincidence with the experimental data. The D^*_{an} data resulting from the RTD measurements are plotted in Figures 4 and 5 as Greek crosses (+).

For the four complexes examined, Figures 4 and 5 reveal the differences between D_σ, D^*_{cat}, and D^*_{an}. It is important to note that the solid lines are not VTF fits; instead, they represent the results of fitting within a comprehensive ion-transport model to be presented in sections 4 and 5. At this stage, the solid lines may also help in recognizing the main experimental findings: (i) The diffusion coefficients of cations and anions (D^*_{cat}, D^*_{an}) are very similar over the complete temperature range, irrespective of the salt concentration and the addition of I_2. This contrasts with corresponding data on PEO-based electrolytes with inorganic salts (LiTFSI,[20] NaI[21]), for which the anion is always faster than the cation. (ii) The charge diffusivity D_σ is smaller than the diffusion coefficients of the individual ions. In particular, D_σ distinctly falls below the sum of D^*_{cat} and D^*_{an}, which points to significant ionic aggregation. (iii) In $PEO_{30}PMImI$ and $PEO_{30}PMImI:I_2$, the three distinct diffusion coefficients appear to follow parallel curves. By contrast, in $PEO_{20}PMImI$ and $PEO_{20}PMImI:I_2$ the Arrhenius plot of D_σ exhibits a stronger curvature than the mutually similar curvatures of D^*_{cat} and D^*_{an}, thus leading to greater disparities at high T. This indicates that the T dependence of ion pairing is weak in the more diluted system (y = 30) but appreciably stronger in the more concentrated system (y = 20). (iv) In both systems, the I_2 addition leads to an enhancement of all three diffusivities, as revealed by comparing Figure 4a with Figure 4b and Figure 5a with Figure 5b. However, the increase of D_σ is much larger than that of D^*_{cat} and D^*_{an}. The magnitudes of the relative changes are specified in Table 1.

The above observations will be evaluated within a theoretical framework that has been described in detail in previous publications.[10,11,22] To this aim, the underlying ideas and

dx.doi.org/10.1021/jp303579b | J. Phys. Chem. B 2012, 116, 8290−8298

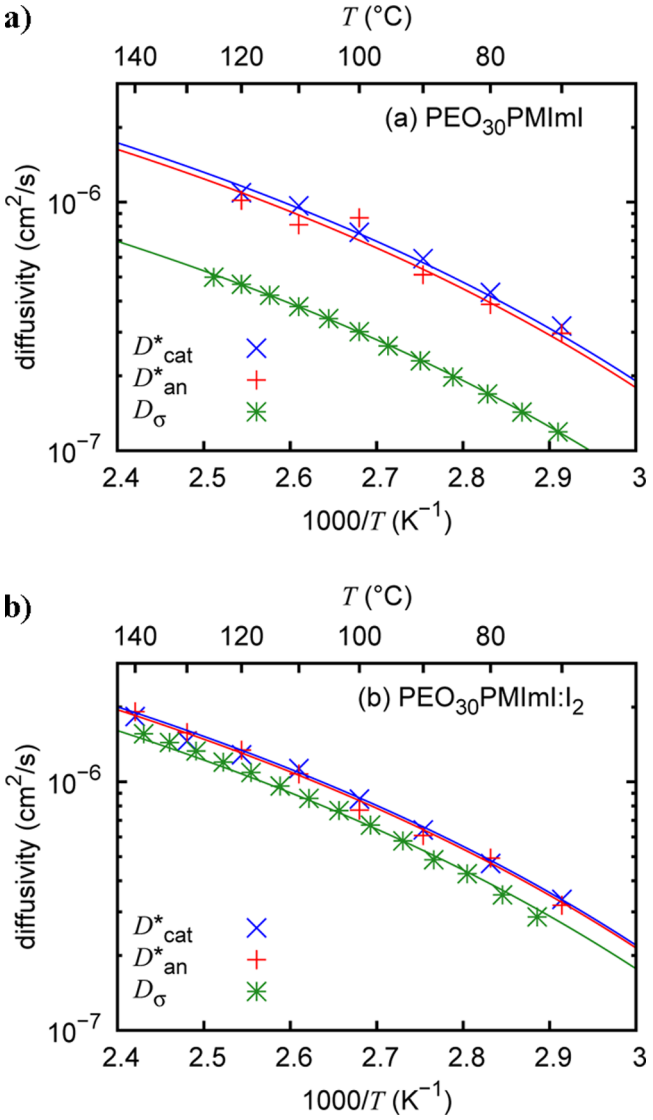

Figure 4. Diffusion coefficients D^*_{cat}, D^*_{an}, and D_σ in $PEO_{30}PMImI$ (a) and $PEO_{30}PMImI:I_2$ (b) as a function of inverse temperature, as indicated. The solid lines represent a simultaneous fit of all experimental data on both $PEO_{30}PMImI$ and $PEO_{30}PMImI:I_2$ within the extended model 1.

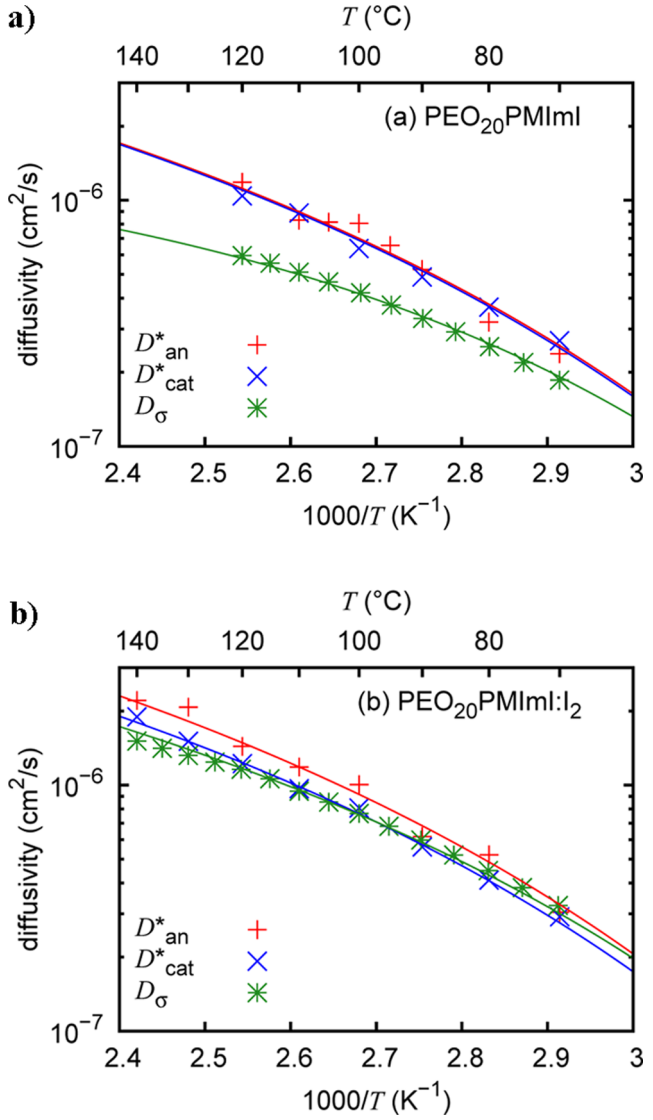

Figure 5. Diffusion coefficients D^*_{cat}, D^*_{an}, and D_σ in $PEO_{20}PMImI$ (a) and $PEO_{20}PMImI:I_2$ (b) as a function of inverse temperature, as indicated. The solid lines represent a simultaneous fit of all experimental data on both $PEO_{20}PMImI$ and $PEO_{20}PMImI:I_2$ within the extended model 1.

relevant equations of the employed ion-transport model will be presented in the next section.

4. ANALYSIS WITHIN AN ION-TRANSPORT MODEL

4.1. Basic Model and Primary Evaluation. In SPE complexes of moderate or low salt concentration, the formation of cation−anion pairs according to the reversible reaction

$$cat^+ + an^- \rightleftharpoons pair \tag{5}$$

appears to be the predominant ion-aggregation process.[23−25] Thus, neglecting higher-order clusters, the cation diffusivity may be written as

$$D^*_{cat} = \hat{D}_{cat^+} + \hat{D}_{pair} \equiv (1 - r_{pair})D_{cat^+} + r_{pair}D_{pair} \tag{6}$$

$$D^*_{an} = \hat{D}_{an^-} + \hat{D}_{pair} \equiv (1 - r_{pair})D_{an^-} + r_{pair}D_{pair} \tag{7}$$

where $r_{pair} = C_{pair}/C_{salt}$ denotes the relative concentration of neutral pairs (or pair fraction). The diffusivities marked with an asterisk (D^*_{cat}, D^*_{an}) are measured by PFG-NMR or RTD and thus represent the total diffusion coefficient of cations or anions, averaged over all relevant mobile species. On the contrary, the plain D symbols (D_{cat^+}, D_{an^-}, D_{pair}) designate the true diffusivities of the individual species (cat^+, an^-, pair), which are related to the respective mobilities. Furthermore, D's labeled with a "hat" ($\hat{D}_{cat^+}$, $\hat{D}_{an^-}$, $\hat{D}_{pair}$) are so-called effective diffusion coefficients which also involve the relative concentration of the respective species (r_{pair} or $1 - r_{pair}$). Thus, in this

Table 1. Relative Diffusivity Increase in Complexes with Added I_2 in Comparison to the Base Complexes without Iodine[a]

	D^*_{cat} (%)	D^*_{an} (%)	D_σ (%)
$PEO_{20}PMImI:I_2$	25	10−15	85
$PEO_{30}PMImI:I_2$	25	10−15	130

[a]The given data are averages over the temperature range 70−120 °C.

dx.doi.org/10.1021/jp303579b | J. Phys. Chem. B 2012, 116, 8290−8298

notation D_σ is given by the sum of the contributions of charged species, i.e.

$$D_\sigma = \hat{D}_{cat^+} + \hat{D}_{an^-} \equiv (1 - r_{pair})D_{cat^+} + (1 - r_{pair})D_{an^-} \quad (8)$$

The left-hand sides of the three equations (6) to (8) comprise three *a priori* unknown variables, viz., $\hat{D}_{cat^+}$, $\hat{D}_{an^-}$, and $\hat{D}_{pair}$. Solving this equation system yields the effective diffusivities as a function of the measured data, i.e.

$$\hat{D}_{cat^+} = \frac{1}{2}(D^*_{cat} - D^*_{an} + D_\sigma) \quad (9)$$

$$\hat{D}_{an^-} = \frac{1}{2}(D^*_{an} - D^*_{cat} + D_\sigma) \quad (10)$$

$$\hat{D}_{pair} = \frac{1}{2}(D^*_{an} + D^*_{cat} - D_\sigma) \quad (11)$$

Then, the relative pair contributions to cation and anion transport, t^{cat}_{pair} and t^{an}_{pair}, can be calculated using eqs 6 and 7 as

$$t^{cat}_{pair} = \frac{\hat{D}_{pair}}{\hat{D}_{cat^+} + \hat{D}_{pair}} = \frac{\hat{D}_{pair}}{D^*_{cat}} \quad (12)$$

$$t^{an}_{pair} = \frac{\hat{D}_{pair}}{\hat{D}_{an^-} + \hat{D}_{pair}} = \frac{\hat{D}_{pair}}{D^*_{an}} \quad (13)$$

Hence, the calculation of t^{cat}_{pair} and t^{an}_{pair}, which may be conceived as pair-related transport numbers of cations and anions, respectively, is a straightforward matter.

The results of these calculations for the electrolytes investigated are presented in Table 2. As indicated before, the impact of neutral pairs to mass transport appears to be strong, since t^{cat}_{pair} and t^{an}_{pair} are higher than 45% in all four complexes. However, a close inspection reveals that the transport numbers in the complexes with additional I_2 are distinctly lower than in the iodine-free complexes. Thus, adding I_2 is found to diminish ion pairing substantially.

Table 2. Relative Pair Contributions to Cation and Anion Transport for Electrolytes with and without I_2 Calculated Using Eqs 12 and 13

	t^{cat}_{pair} (%)	t^{an}_{pair} (%)
$PEO_{20}PMImI$	60–75	65–75
$PEO_{20}PMImI:I_2$	50–70	45–60
$PEO_{30}PMImI$	75–80	80–85
$PEO_{30}PMImI:I_2$	55–65	55–65

4.2. Pair Fractions and True Diffusivities. It is important to distinguish the pair-related transport numbers from the pair fraction r_{pair}. Basically, the same value of, e.g., t^{cat}_{pair} can be obtained either by many slowly diffusing pairs or by few fast-diffusing pairs. Therefore, to split up effective diffusivities in relative abundance (r_{pair} or $1 - r_{pair}$) and true diffusivity (D_{cat^+}, D_{an^-}, or D_{pair}) of the pertaining ionic species, further considerations are necessary. By applying the mass action law to the reaction eq 5, one obtains

$$r_{pair} = 1 + \frac{1}{2k_{pair}}(1 - \sqrt{1 + 4k_{pair}}) \quad (14)$$

The reaction constant k_{pair} is supposed to be thermally activated, so that

$$k_{pair} = k^0_{pair} \exp\left(-\frac{\Delta H_{pair}}{k_B T}\right) \quad (15)$$

holds true. Here ΔH_{pair} represents the pair formation enthalpy while the prefactor k^0_{pair} is a dimensionless quantity[10,26] that can be written as

$$k^0_{pair} = \exp(\Delta S_{pair}/k_B) \quad (16)$$

where ΔS_{pair} stands for the entropy of pair formation. Moreover, it seems reasonable to assume that the true diffusivities can be described by the following VTF equations:

$$D_{cat^+} = D^0_{cat^+} \exp\left(-\frac{B_{cat^+}}{T - T_0}\right) \quad (17)$$

$$D_{an^-} = D^0_{an^-} \exp\left(-\frac{B_{an^-}}{T - T_0}\right) \quad (18)$$

$$D_{pair} = D^0_{pair} \exp\left(-\frac{B_{pair}}{T - T_0}\right) \quad (19)$$

Here we take it for granted that T_0 is independent of the respective species but that most generally the B parameters and the prefactors D^0 may be all different.

The above expressions for the true diffusivities and r_{pair} can be inserted in eqs 6–8 to give a complete description of ionic transport in each electrolyte separately. This requires for each electrolyte nine independent parameters, i.e., ΔH_{pair}, k^0_{pair}, B^-_{an}, B^+_{cat}, B_{pair}, $D^0_{an^-}$, $D^0_{cat^+}$, D^0_{pair}, and T_0. Best values for these parameters can be obtained by simultaneously fitting the three expressions (6) to (8) to the three sets of experimental data. However, with these nine parameters the degree of freedom proved to be too large to obtain statistically reliable results. Therefore, additional assumptions are needed to reduce the number of free parameters.

4.3. Specification of Distinct Submodels. In earlier work by our group on PEO-based SPEs with inorganic salts, constraining assumptions regarding the model parameters were made either intuitively[10] or on the basis of molecular dynamics (MD) simulations[21] reported by others.[27] However, the situation may be different for PEO–salt complexes containing ionic liquids with their bulky organic cations. Therefore, we examined in this study by trial-and-error up to five different submodels with specific assumptions concerning the correlations among the diffusivities of anions, cations, and pairs. Such correlations can either exist in terms of a shared temperature dependence (same B values) or in terms of a common diffusivity (same B and D^0 values). One submodel, to be termed model 1 henceforward, requires the temperature dependence to be equal for all three mobile species, leading to

$$B_{cat^+} = B_{an^-} = B_{pair} \quad (20)$$

Another submodel, designated as model 2, was based on the idea that cations and pairs may have the same diffusivity; thus[28]

$$D^0_{pair} = D^0_{cat^+} \quad (21)$$

$$B_{pair} = B_{cat^+} \quad (22)$$

dx.doi.org/10.1021/jp303579b | J. Phys. Chem. B 2012, 116, 8290–8298

Table 3. Parameter Values and Their Statistical Error Obtained for Two PEO_yPMImI:I_2(1:z) Systems from Simultaneous Fitting of the Experimental Data for $z = 0$ and $z = 1/4$ within the Extended Model 1

	ΔS_{pair} (k_B)	ΔH_{pair} (eV)	$D^0_{cat^+}$ (10^{-5} cm^2 s^{-1})	$D^0_{an^-}$ (10^{-5} cm^2 s^{-1})	D^0_{pair} (10^{-5} cm^2 s^{-1})	B (K)	T_0 (K)
$y = 20$	10.3 ± 0.3	0.23 ± 0.01	5.8 ± 1.0	6.2 ± 1.0	3.1 ± 0.6	563 ± 40	231 ± 6
$y = 30$	4.0 ± 0.03	0.0 ± 0.001	6.4 ± 1.5	4.8 ± 1.0	3.2 ± 0.6	597 ± 50	219 ± 5

A third submodel, just to make clear the wide spectrum of models tested, stipulates the equality of the cation and anion diffusivity ($B_{cat^+} = B_{an^-}$ and $D^0_{cat^+} = D^0_{an^-}$), etc.

With most tested submodels the experimental results can be satisfactorily described, as confirmed by the relatively small deviations from the best fits obtained for the individual electrolytes. Thus, even with a reduced number of parameters (6 or 7 instead of 9) there are still too many degrees of freedom to clearly discriminate between the submodels. It should be emphasized that all tested submodels consistently reproduce the effective diffusivities and the pair-related transport numbers as compiled in Table 2.[29] Nevertheless, the overall result is unsatisfying as it does not allow for a justified choice of the physical conditions that are most likely prevailing. Therefore, to get meaningful results, we implemented a more elaborate treatment that relied on the similarities between electrolytes of the same salt concentrations. Thus, the complexes PEO_yPMImI and PEO_yPMImI:I_2 with equal y value were simultaneously fitted within an extended model, in which the differences due to dissimilar I_2 contents mainly result from changes in ion-pairing behavior.

5. COMBINED ANALYSIS WITHIN AN EXTENDED ION-TRANSPORT MODEL

In this section we recapitulate the main features of a previously developed model for polymer/iodide-salt complexes with varying amounts of added iodine.[11]

When adding I_2 to a polymer electrolyte containing an iodide such as, e.g., PMImI as salt, both iodine-related species may react according to

$$I_2 + I_1^- \rightarrow I_3^- \tag{23}$$

It has been reported that to a good approximation I_2 fully transforms to I_3^-.[7,15] As the diffusivities of I_1^- and I_3^- are found to be similar in magnitude for a variety of related systems,[3] it is explicitly assumed here that $D_{I_3^-} = D_{I_1^-} = D_{an^-}$. More speculatively, we also assume that I_3^- does not take part in pair formation at all. Nevertheless, this seems reasonable as the triiodide ion has an asymmetric bulky shape and a delocalized charge.[11] All other parameters, i.e., the diffusivity of ions and pairs and the ion-pairing parameters of the monoiodide ion, are supposed to be the same in complexes with the same composition parameter y. Based on these assumptions, the main effect of the I_2 additive will be that the pair fraction changes to lower values. The key question is, however, whether this whole set of physical constraints leads to quantitatively satisfactory description of the experimental data.

The implementation of the above considerations in the original ion-transport model requires some modifications, which have been derived in a previous paper.[11] First, the I_2/salt-molecule molar ratio z enters the mathematical formalism of the extended model as additional parameter. Second, the pair fraction then changes to

$$r_{pair} = 1 - z/2 + \frac{1}{2k_{pair}} \left(1 - \sqrt{1 + 4k_{pair}(1 - z/2) + (k_{pair} z)^2}\right) \tag{24}$$

Third, due to the higher amount of iodine the diffusion coefficient of the anions has to be written as[30]

$$D^*_{an} = \frac{1}{1 + 2z}((1 - r_{pair} + 2z)D_{an^-} + r_{pair} D_{pair}) \tag{25}$$

Except for these modifications, the same expressions as given in the previous section are used.

Without any further assumptions, we have nine parameters for a combined description of complexes with the same salt concentration. Similarly as before, the earlier discussed submodels can be used to reduce the number of free parameters even further. Remarkably, in contrast to the fitting of single complexes described in the previous section, it is found that most of the tested submodels are not able to reproduce the measured data. This is, for example, easy to understand in the case when the free cation is assumed to have the same true diffusivity as the pairs (model 2, see previous section). In such a situation, D^*_{cat} does not depend on the pair concentration and therefore is not influenced by adding I_2 (cf. eq 6). This, however, contradicts the experimental observation that D^*_{cat} is higher in complexes with additional I_2.

Interestingly, it is found that only one particular submodel can well reproduce the experimental results both in the systems with $y = 20$ and $y = 30$. This successful submodel is model 1, i.e., the one with the same temperature dependence ($B_{an^-} = B_{cat^+} = B_{pair}$) but different magnitudes ($D^0_{cat^+} \neq D^0_{an^-} \neq D^0_{pair}$) of the true diffusivities. The results of fitting are shown in Figures 4 and 5. The optimized parameters obtained by this model are compiled in Table 3 and discussed in the next section.

6. DISCUSSION

6.1. Model Fitting and Parameter Values. The present approach grounds on the idea to describe the experimental observations with a minimum number of free parameters. Indeed, it proved possible to obtain good fits with seven free parameters for both PEO−PMImI systems, comprising in either case a complex with iodine and a corresponding iodine-free base complex. The quality of the fits is revealed in Figures 4 and 5 and quantified by the mean deviations of the data points from the best fit, amounting to about 5% for either system. The usefulness of our concepts is further sustained by the narrow error limits of the parameter values listed in Table 3. Altogether, seven parameters are needed to reproduce six individual sets of T-dependent experimental data (D^*_{cat}, D^*_{an}, and D_σ for two complexes with the same reduced salt concentration y). Thus, on the average somewhat more than one free parameter (i.e., 7/6) is required for each diffusivity as a function of temperature. For comparison, a "model-free" VTF fit would require three parameters for each diffusivity.

The fact that model 1 yields the best fitting results implies that all ionic species undergo the same relative changes in

dx.doi.org/10.1021/jp303579b | J. Phys. Chem. B 2012, 116, 8290−8298

mobility with variations in temperature (cf. eqs 17−20). This is indicative of a strongly correlated system, in which the transport properties (diffusivity, microviscosity) are intimately connected with the segmental motion of the polymer chains. The successful application of model 1 complies with the experimental finding $D^*_{cat} \approx D^*_{an}$, which points to a weak coordination of the polymer to the cation. This is in contrast to the situation in PEO-based electrolytes complexing an inorganic salt such as, e.g., NaI, for which $D^*_{cat} < D^*_{an}$ is observed. In the latter case, the strong cation−polymer binding in conjunction with a weak anion−polymer interaction appears to be consistent with the validity of model 2,[11,21] which allows for a partly decoupling of anionic motion (cf. eq 21). The above views and findings are corroborated by the results of MD simulations on similar PEO-based systems with inorganic salts[27] and ionic liquids.[31,32]

As the diffusivity of all mobile species have the same T dependence ($B_{cat^+} = B_{an^-} = B_{pair}$), the proportions between their magnitudes are expressed by the pre-exponential factors $D^0_{cat^+}$, $D^0_{an^-}$, and D^0_{pair}. It is seen in Table 3 that within each system the free cations and anions have a similarly high diffusivity, whereas the pairs move only about half as fast as the faster type of free ion ($D_{pair} \approx 0.5 \times \max(D_{cat^+}, D_{an^-})$). Also, the similarities between the systems, including the values of B and T_0, reflect the relatively small differences in ionic transport between the compositions with $y = 30$ and 20. However, great disparities are found for ΔH_{pair} and $\Delta S_{pair}/k_B = \ln k^0_{pair}$. The enthalpy $\Delta H_{pair} = 0$ obtained for the more dilute system ($y = 30$) implies a very weak T dependence of ion pairing, which relates to the almost parallel alignment of D^*_{cat}, D^*_{an}, and D_σ in Figure 4a,b. By contrast, $\Delta H_{pair} = 0.23$ resulting for the more concentrated system ($y = 20$) gives rise to increasing pair formation with increasing T, which produces a diverging curve toward high T in Figure 5a,b.

Since the experiments show that $D^*_{cat} \approx D^*_{an}$ approximately holds over the temperature range of interest, it does not surprise that modeling yields $D_{cat^+} \approx D_{an^-}$. For the $PEO_{30}PMImI/PEO_{30}PMImI:I_2$ system, D_{an^-} varies from 2.2×10^{-6} cm^2 s^{-1} at 140 °C to 3.9×10^{-7} cm^2 s^{-1} at 70 °C (cf. eq 18 and Table 3). Also, the finding that the ion pair moves slower than either of its constituent ions seems plausible. Furthermore, $T_0 = 231$ K for $y = 20$ is somewhat larger than the corresponding value (219 K) for $y = 30$, thus following the usual trend with increasing salt concentration.[21,33] A reverse trend is found for the B parameter, also in agreement with reports on conventional SPE systems.[21] It has to be admitted, however, that both trends are not statistically significant. Although the two ΔH_{pair} results greatly differ, the corresponding r_{pair} values (cf. eq 14) are similar in magnitude. This is illustrated by the two upper lines in Figure 6. $\Delta H_{pair} \approx 0$ obtained for $y = 30$ results in $r_{pair} \approx 0.88$ for $PEO_{30}PMImI$ independent of T. By contrast, r_{pair} related to $PEO_{20}PMImI$ does show a T dependence, which according to eqs 14 and 15 remains from a much stronger T dependence of k_{pair}.

6.2. Effects of Iodine Addition. The effect of I_2 addition is also manifest in Figure 6 (cf. two lower lines). For $PEO_{30}PMImI:I_2$ the pair fraction is reduced from 0.88 mentioned above to a constant value of about 0.70. A similar downshift of r_{pair} with respect to the base complex is observed for $PEO_{20}PMImI:I_2$. The pair fraction decreases because I_2 binds to the I_1^- ions, thereby diminishing the number of anions capable of forming pairs with $PMIm^+$. The reduction of r_{pair} goes along with an increase of the fraction of free ions $1 - r_{pair}$.

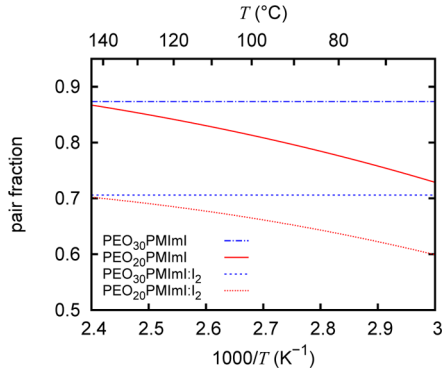

Figure 6. Pair fraction r_{pair} as a function of inverse temperature for PEO_yPMImI and $PEO_yPMImI:I_2$ complexes of different composition y, as indicated. Solid line and chain line: base complexes without iodine. Dashed lines: complexes with iodine as additive.

This leads to the observed enhancement of D_σ, which according to eq 8 is proportional to $1 - r_{pair}$. However, also D^*_{cat} and D^*_{an} profit from the lowering of r_{pair}, as it favors the free-ion term at the cost of the pair term in eqs 6 and 7. The argument counts because data fitting consistently yields that the free ions move faster than the pair, as discussed above, i.e., D_{cat^+}, $D_{an^-} > D_{pair}$.

The low ion-pairing propensity of I_3^- can be understood from the bulky character of the anion and the concomitant delocalization of the electric charge. The latter effect leads to a weak Coulombic binding to the cation and hence a higher pair-formation enthalpy than ΔH_{pair} for pairs of $PMIm^+$ and I_1^-. Moreover, the bulky and less symmetric shape of the I_3^- ion reduces the number of preferable bond states with the cation, which translates to a lower entropy gain upon pairing. Both effects, a high enthalpy and a low entropy of $PMIm^+$−I_3^- pairing, disfavor this kind of ion association.

The low pairing tendency of I_3^- seems also consistent with the stabilizing effect of I_2 addition to the PEO_yPMImI electrolytes mentioned in section 2. The formation of I_3^- according to the reaction given by eq 23 may prevent the precipitation of the PMImI ionic liquid at temperatures above 120 °C. This entropy-driven process[34] was indicated by DSC and EIS analysis of the base complexes, but it was not observed anymore in $PEO_{20}PMImI:I_2$ and $PEO_{30}PMImI:I_2$ up to the highest temperature investigated being near 150 °C. One possibility is that the bulky I_3^- entities of low symmetry cannot be favorably incorporated in the pure ionic liquid, thus causing upshifting of the critical precipitation temperature. Additionally, the precipitation process may be kinetically hampered due to the occurrence of virtually nonpairing I_3^- ions since it seems plausible that ion pairing constitutes an initial step in the formation of salt nuclei.

It is noteworthy that the crucial effect of I_2 addition appears to be a reduced fraction of neutral pairs. To explain the experimental data, it is not necessary to introduce an additional Grotthuss-like transport mechanism, which would involve the exchange of an I_2 molecule between I_3^- and I_1^- ions.[13−15] This agrees with the finding that this mechanism can only operate at high iodide concentrations such as, e.g., encountered in undiluted ionic-liquid iodides, where the average distance between adjacent I_3^- and I_1^- ions is sufficiently small.[35] Furthermore, the Grotthuss mechanism on its own could only explain the small increase of D^*_{an} but not the strong enhancement of D_σ observed experimentally (cf. Table 1).

dx.doi.org/10.1021/jp303579b | J. Phys. Chem. B 2012, 116, 8290−8298

6.3. Comparison with the PEO−NaI System. Remarkable is not so much the fact that the ΔH_{pair} values are significantly different for the examined PEO−IL systems with y = 30 and y = 20, as similar differences were found between $PEO_{30}NaI$ ($\Delta H_{pair} \approx 0.2$) and $PEO_{20}NaI$ ($\Delta H_{pair} \approx 0.0$).[11,21] What surprises most is the reverse order in magnitude as a function of salt concentration, since for PEO_yPMImI the lower ΔH_{pair} value (~0) pertains to the more dilute composition (y = 30). This small enthalpy seems to comply with the weak coordination of the polymer to the cation and with the charge delocalization on $PMIm^+$. However, the strong increase of ΔH_{pair} upon a 50% increase in salt concentration, i.e., from 1/30 to 1/20 in terms of $1/y$, is presently not clear. We tentatively propose that ionic structuring in a concentrated system may play a role here. This may relate to the intermediate-range order found by MD simulations on similar SPE−IL systems.[31]

Despite the large difference in ΔH_{pair} between $PEO_{30}PMImI$ and $PEO_{30}NaI$, the r_{pair} values at 140 °C are not too far apart (0.88 versus 0.72,[11] respectively). This is due to compensating differences in ΔS_{pair} (cf. Table 3). However, the discrepancy increases with decreasing temperature (e.g., 0.88 versus 0.56 at 70 °C). In both systems, the relative decrease in r_{pair} caused by the addition of I_2 (same molar fraction, i.e., z = 1/4) amounts to about 20% (cf. Figure 6 with Figure 4 in ref 11). Thus, the iodine effect appears to be consistent among PEO-based electrolytes with different kinds of iodide salt.

Also, other results of the present work can be directly compared with corresponding data for PEO−NaI.[11,21] Specifically, in $PEO_{30}PMImI$ the experimental diffusivity D^*_{an} is larger by a factor of ~2 with respect to $PEO_{30}NaI$ over the same temperature range while for the disparity amounts to factors of 4 (140 °C) to 10 (70 °C). However, comparing the true diffusivities of individual species, it turns out that D_{an^-} is similarly large in the two systems (within 20%), whereas $PMIm^+$ is faster than Na^+ by factors ranging from 7.5 (140 °C) to 18 (70 °C).[11,21] In view of the fact that T_0 does not change within error limits (219 K versus 216 K), this comparison shows that a major difference between $PEO_{30}PMImI$ and $PEO_{30}NaI$ concerns the cation mobility.

For PEO_yNaI electrolytes the increase in salt concentration from y = 30 to y = 20 appears to be accompanied by the transition to a two-phase region in the phase diagram.[21,36] In this region, highly concentrated PEO_3NaI crystallites are formed within an amorphous PEO−NaI matrix whose composition is given by the liquidus line. Although such data are not available for the PEO−PMImI system, the step from $PEO_{20}PMImI$ to $PEO_{30}PMImI$ may imply entering into a virtually high-concentration regime. Based on the size of the cation, such a transition may even take place at a lower critical salt concentration than in PEO−NaI. It is worth noting that we were not able to obtain reproducible results for the T-dependent conductivity σ in $PEO_{10}PMImI$, which may indicate the occurrence of slow precipitation processes in this yet more concentrated complex. In addition, there seems to be a fundamental difference between charge transport in highly concentrated ionic systems such as ILs and in (polymer) electrolyte solutions where ionic motion takes place within a medium.[37] Thus, for further studies on ionic transport in PEO−IL systems, both the regimes of high and low salt concentration seem interesting, i.e., high concentrations rather for their great technological relevance and low concentrations to focus on fundamental issues of ion mobility and ion pairing.

7. CONCLUSIONS

This study on polymer electrolytes with an ionic-liquid iodide as salt component provides crucial insight into the characteristics of ionic transport in potential electrolytes for dye-sensitized solar cells. A special feature is the use of ^{125}I radiotracer diffusion, which is the only method capable of directly monitoring long-range motion of iodine ions in soft-matter systems. Combining the radiotracer technique with PFG-NMR to determine the cation diffusivity and with impedance spectroscopy to measure the overall ionic conductivity yields a virtually complete experimental picture of mass and charge transport in $PEO_{20}PMImI$ and $PEO_{30}PMImI$ complexes with and without I_2 as additive.

It is found that the cation and anion diffusivity are of closely similar magnitude and thus exhibit a similar temperature dependence. About 50% or more of ionic mass transport is due to neutral pairs, whereas charge transport suffers from the strong ion-pairing tendency. However, the addition of free iodine leads both to a small increase of mass transport and a strong enhancement of charge transport. This behavior can be fully explained by the formation of the bulky I_3^- ion and its reduced propensity to form pairs with the $PMIm^+$ cations.

The experimental data are best described within a model that assumes weak binding of the cation to the polymer chains and concomitantly a strong dynamic coupling of all mobile species among each other. The mobility of pairs appears to be about half as high as that of the charged free cations and anions. The major differences between $PEO_{20}PMImI$ and $PEO_{30}PMImI$ concern the enthalpy and entropy of pair formation as reflected by the dissimilar variations of the pair fraction and the charge diffusivity with temperature. These results on ionic-liquid polymer electrolytes differ in detail from classical SPE systems with inorganic salts. A better understanding of ion transport may be obtained in future investigations by covering a wider composition range including more dilute (i.e., IL-in-polymer) and more concentrated (i.e., polymer-in-IL) systems.

AUTHOR INFORMATION

Corresponding Author

*E-mail: stolwij@uni-muenster.de. Phone: +49 (0)251 8339013. Fax: +49 (0)251 8338346.

Notes

The authors declare no competing financial interest.

ACKNOWLEDGMENTS

The authors thank Sebastian Jeremias for help in preliminary PFG-NMR experiments. Financial support by the Deutsche Forschungsgemeinschaft is gratefully acknowledged.

REFERENCES

(1) Ueno, K.; Tokuda, H.; Watanabe, M. *Phys. Chem. Chem. Phys.* **2010**, *12*, 1649−1658.

(2) Kim, H.; Ding, Y.; Kohl, P. A. *J. Power Sources* **2012**, *198*, 281−286.

(3) Zakeeruddin, S. M.; Grätzel, M. *Adv. Funct. Mater.* **2009**, *19*, 2187−2202 . Table 4 of this article presents a compilation of literature data showing that $0.5 < D_{I_3^-}/D_{I_1^-} < 2$ holds in all cases, in which both diffusion coeffients were determined, with one exception.

(4) Shin, J.-H.; Henderson, W.; Appetecchi, G.; Alessandrini, F.; Passerini, S. *Electrochim. Acta* **2005**, *50*, 3859−3865.

(5) Freitas, F. S.; de Freitas, J. N.; Ito, B. I.; De Paoli, M.-A.; Nogueira, A. F. *Appl. Mater. Interfaces* **2009**, *12*, 2870−2877.

(6) Grätzel, M. *Inorg. Chem.* **2005**, *44*, 6841−6851.

(7) Kawano, R.; Watanabe, M. *Chem. Commun.* **2003**, 330−331.
(8) Kalaignan, G. P.; Kang, M.-S.; kang, Y. S. *Solid State Ionics* **2006**, *177*, 1091−1097.
(9) Singh, P. K.; Kim, K.-W.; Rhee, H.-W. *Polym. Eng. Sci.* **2009**, *49*, 862−865.
(10) Stolwijk, N. A.; Obeidi, S. *Phys. Rev. Lett.* **2004**, *93*, 125901.
(11) Call, F.; Stolwijk, N. A. *J. Phys. Chem. Lett.* **2010**, *1*, 2088−2093.
(12) Stolwijk, N.; Wiencierz, M.; Fögeling, J.; Bastek, J.; Obeidi, S. *Z. Phys. Chem.* **2010**, *224*, 1707−1733.
(13) Ruff, I.; Friedrich, V. J.; Csillag, K. *J. Phys. Chem.* **1972**, *76*, 162−165.
(14) Kawano, R.; Watanabe, M. *Chem. Commun.* **2005**, *16*, 2107−2109.
(15) Papageorgiou, N.; Athanassov, Y.; Armand, M.; Bonhôte, P.; Pettersson, H.; Azam, A.; Grätzel, M. *J. Electrochem. Soc.* **1996**, *143*, 3099−3108.
(16) According to the lot specifications, the base PEO material typically contained 1.4 wt % SiO_2 and 0.2 wt % CaO. These contaminations are inherent to the manufacturing process and present in the form of small particles.
(17) Obeidi, S.; Zazoum, B.; Stolwijk, N. *Solid State Ionics* **2004**, *173*, 77−82.
(18) Stolwijk, N. A.; Wiencierz, M.; Heddier, C.; Kösters, J. *J. Phys. Chem. B* **2012**, *116*, 3065−3074.
(19) Tanner, J. E. *J. Chem. Phys.* **1970**, *52*, 2523−2526.
(20) Orädd, G.; Edman, L.; Ferry, A. *Solid State Ionics* **2002**, *152*−*153*, 131−136.
(21) Wiencierz, M.; Stolwijk, N. A. *Solid State Ionics* **2012**, *212*, 88−99.
(22) Fögeling, J.; Kunze, M.; Schönhoff, M.; Stolwijk, N. A. *Phys. Chem. Chem. Phys.* **2010**, *12*, 7148−7161.
(23) Bruce, P. E. *Solid State Electrochemistry*; Cambridge University Press: Cambridge, UK, 1997.
(24) Schantz, S. *J. Chem. Phys.* **1991**, *94*, 6296−6306.
(25) Stolwijk, N.; Wiencierz, M.; Obeidi, S. *Electrochim. Acta* **2007**, *53*, 1575−1583.
(26) Stolwijk, N. A.; Obeidi, S. *Defect Diffus. Forum* **2005**, *237*−*240*, 1004−1015.
(27) Maitra, A.; Heuer, A. *J. Phys. Chem. B* **2008**, *112*, 9641−9651.
(28) The designation as model 1 (or original model) and model 2 (or modified model) has historical reasons; see ref 22.
(29) This is a consequence of the fact that eqs 9−13 hold true independently of the specific submodel assumptions.
(30) Here it is assumed that the forward and backward reaction rates establishing dynamic equilibrium among the iodine species according to eq 23 are sufficiently fast on the time scale of a radiotracer diffusion experiment (typically ∼1 h).
(31) Costa, L. T.; Ribeiro, M. C. *J. Chem. Phys.* **2006**, *124*, 184902/1−8.
(32) Costa, L. T.; Ribeiro, M. C. *J. Chem. Phys.* **2007**, *127*, 164901/1−7.
(33) Perrier, M.; Besner, S.; Paquette, C.; Vallee, A.; Lascaud, S.; Prud'homme, J. *Electrochim. Acta* **1995**, *40*, 2123−2129.
(34) Bastek, J.; Stolwijk, N.; Köster, T. K.-J.; van Wüllen, L. *Electrochim. Acta* **2010**, *55*, 1289−1297.
(35) Cao, Y.; Zhang, J.; Bai, Y.; Li, R.; Zakeeruddin, S. M.; Grätzel, M.; Wang, P. *J. Phys. Chem. C* **2008**, *112*, 13775−13781.
(36) Fauteux, D.; Lupien, M.; Robitaille, C. *J. Electrochem. Soc.* **1987**, *134*, 2761−2766.
(37) Kashyap, H.; Annapureddy, H.; Raineri, F.; Margulis, C. *J. Phys. Chem. B* **2011**, *115*, 13212−13221.